DX.DOI.ORG//10.19199/2023.169.1121-9041.036

Study on fine soil behaviour in function of temperature in the context of climate change

Jérémy Jean Daniel Torche*
Erika Prina Howald*

* School of Engineering and Management Vaud (HEIG-VD), Institute Insit, Yverdon-les-Bains, Switzerland

Corresponding author:
erika.prinahowald@heig-vd.ch

One of the expected effects of global warming is the gradual melting of permafrost. Its melting will significantly impact soil material properties, potentially causing instability of infrastructures and triggering natural hazards.
The objective of this experimentation is to quantify the effect of thawing on the geomechanical strength of a reconstituted fine soil. More specifically, it is intended to qualify the initial frozen state and compare it to the state after thawing. This study was carried out in three steps. To begin, soil samples were identified by the usual parameters. Then, artificial samples were sheared at a temperature of –5°C in our temperature controlled triaxial press in order to determine the soil's parameters. Finally, identical tests were carried out at a temperature of +5°C in order to thaw the soil completely before the shearing. In total, three tests for each temperature were compared and discussed. The expected results aim at a better understanding and quantification of soil strength reduction after the thawing phase. As many infrastructures are now built on permafrost, such as infrastructures, or alpine chalets, they will be affected by this phenomenon in the near future. A better understanding of (geo)mechanical consequences might facilitate risk analysis, evaluation and mitigation.
Keywords*: climate change, temperature controlled triaxial test, permafrost.*

1. Introduction

The thawing of permafrost has a lot of consequences, not just for the strength of the ground, but also for the structures and infrastructures built on it. Indeed, the variation in ground resistance during the thawing process can lead to a loss of bearing capacity, causing failure of man-made installations and an increase in the frequency of natural hazards. Therefore, this can have an impact on the life of the community.

Permafrost refers to land where the temperature does not exceed 0 °C for at least one year. There are several categories of permafrost:

- Continuous permafrost (more than 80% of the surface area)
- Discontinuous permafrost (between 30% to 80% of the surface area)
- Sporadic permafrost (less than 30% of the surface area)

Permafrost covers around 20% of continental surfaces, mainly at high latitudes (Arctic polar zone, including Greenland, Arctic Siberia, Alaska and northern Canada). Discontinuous permafrost can also be found in the Alps above 2,500 meters and continuous permafrost above 3,500-4,000 meters.

As the impacts of climate change have become increasingly visible over the last few decades, research has been stepped up around the world. Zhang & al. conducted studies on the response of Canadian permafrost after a rise of aerial temperature. The simulation results showed that, at a depth of 0.2 m, a permafrost temperature increase of 2.1 °C, respectively 5.1 °C was expected, for and aerial temperature increase of 2.8 °C, respectively 7 °C (Zhang, *et al.*, 2008). Several predictions of global warming tend to an increase of air temperature to 2 °C to 4 °C in 2100 (Hipp, *et al.*, 2011; Guo, *et al.*, 2012; Lyon, *et al.*, 2022). The temperature of the permafrost will follow the increase of the air temperature. This rise in the soil's temperature progressively shrinks the extent of permafrost and increases the danger areas.

The permafrost degradation due to the global warming effect has a large incidence on natural hazards incurring in mountains such as debris flows, landslides, rock falls, etc. (Haeberli, 1992; Isaksen, *et al.*, 2001; Isaksen, *et al.*, 2002; Etzelmüller, *et al.*, 2003; Isaksen, *et al.*, 2011; Farbrot, *et al.*, 2013; Blikra & Christiansen, 2014; Myhra, *et al.*, 2017; Frauenfelder, *et al.*, 2018; Matthews, *et al.*, 2018) (Prina Howald, *et al.*, 2016). Risk maps have been drawn up in Russia, based on the effects of global warming on permafrost (Perov, *et al.*, 2017). Other studies (Saemundsson, *et al.*, 2018; Sattler, *et al.*, 2011; Stoffel, *et al.*, 2011; Damm & Felderer, 2013; Bardou, *et al.*, 2011) pointed out the impact of degrading permafrost on the triggering of debris flows. The evolution of the rocky glacier dynamics due to the rise of the temperature (Arenson, *et al.*,

If there are references to colour figures in the text, the articles are available in open-access mode on the site www.geam-journal.org

2002) can explain the frequency and amplitude increase of the debris flows. Similar studies have been conducted in China (Ding, *et al.*, 2019) and in the Norwegian sub-arctic permafrost (Hilger, *et al.*, 2021). This degradation is clearly discernible in mountainous countries. For example, in Switzerland we observe the gradual permafrost thawing, thus increasing its instability. This instability can manifest itself by very impressive phenomena such as the collapse of Piz Cengalo in 2017 causing the death of eight people. Another less dramatic issue is the melting of the Theodule glacier. This has caused diplomatic problems between Switzerland and Italy. In fact, the Italian-Swiss border follows the water divide, with the north flowing into Switzerland and the south flowing into Italy. Between 1973 and 2010, the Theodule glacier lost almost a quarter of its mass. This has altered the watershed, forcing the two governments to redraw a few dozen meters of border. Moreover, this border shift has had the effect of "moving" an Italian refuge to Switzerland. The case of the Matterhorn Guides refuge was the subject of intense diplomatic negotiations for over three years in order to reach an agreement between Italy and Switzerland. On top of that, as the risk of falling rocks increases with the thawing of permafrost, many hiking trails close for the safety of people. This closure impacts the local economy.

The consequences of the thaw can have several direct or indirect repercussions for society, which is why it is important to study and understand this phenomenon.

The study of permafrost in Switzerland is an active field of research, mainly since the '70s. A triggering fact was the instability of the ice-saturated scree slopes of the Grande Dixence hydroelectric plant. The study of the phenomenon is very complex and covers many aspects. Chamberlain & Gow have studied in 1979 the evolution of the permeability of four fine-grained soils after a cycle of freeze / thaw. The results are surprising as it was found that the void ratio decreases and the vertical permeability increases. The process depends on the type of soil and no definite relationships have been established (Chamberlain & Gow, 1979). Scientists have also conducted studies on the formation of ice lenses during freezing (Dysli, 1993) and on the evolution of isotherms during freezing, the heat transfers, the water flow during the formation of the ice lenses, the evolution pressures / capillary suctions or the swelling of the ground.

Arenson, Johanson and Springman have proposed mathematical formulations to describe the thermomechanical behavior of ice-rich frozen soils at temperatures close to 0 °C. They highlighted how ice content influences the apparent cohesion and the angle of internal friction. Moreover, apparent cohesion seems to be influenced by the temperature and the applied compression strain rate (Arenson & Springman, 2005). However, only limited analyses of apparent cohesion and friction angle have been carried out and further work is required.

In this paper, a series of temperature-controlled triaxial tests were performed at different temperatures with the aim of simulating the effect of thawing on permafrost. The samples were prepared artificially in order to ensure controlled and repeatable conditions. Thus, only the temperature variable varied during tests. The focus of the investigation presented in this paper was to determine the effect of temperature on the evolution of cohesion and the internal friction angle when samples of fine soil transition from a frozen state to a thawed state.

2. Current state of the applicants' research

Preliminary studies have been carried out on changes in soil strength parameters in order to assess the loss of bearing capacity of permafrost when it thaws (Torche & Prina Howald, 2017; Prina Howald & Torche, 2020). Direct shear tests at the Casagrande box and oedometer tests were performed on silty soils before, during and after a 15-day freezing phase at –15 °C. The result was an increase in soil compressibility of around 40% between soil in its natural state and soil that had undergone a freeze-thaw cycle. In addition, we estimated changes in the soil's angle of internal friction and cohesion by conducting direct shear tests using Casagrande box on samples that were initially frozen at –15 °C and then thawed. However, as the equipment used was not fully adapted to this type of protocol, the test conditions could not be fully controlled.

This preliminary study carried out at the HEIG-VD (High School of Engineering and Management of the canton of Vaud) in Switzerland has shown that soil properties are strongly affected by its physical state (frozen / unfrozen). In fact, the structure of the soil is significantly altered when it freezes. Figures 1 and 2 show the results of tomographic analysis of samples of silty-clay soil with sand and gravel in the frozen state and before freezing. The effect of frost on the structure of the soil is clearly visible.

Although the effects of frost on geomechanical parameters have been shown, the results obtained lack precision.

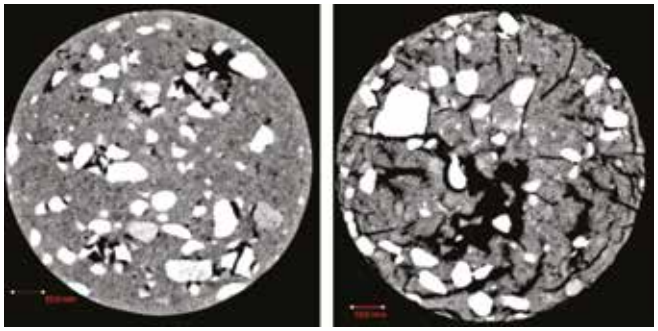

Fig. 1 – Unsaturated A sample section before and during freezing.

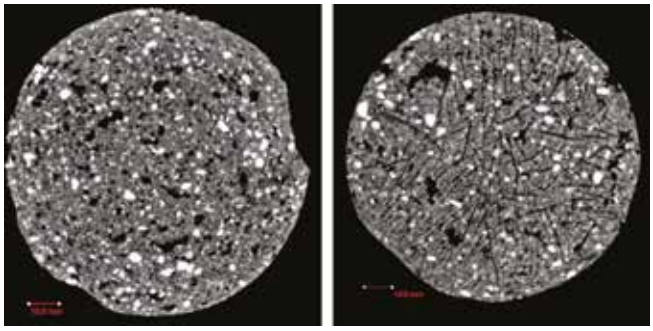

Fig. 2 – Saturated sample B section before and during freezing.

3. Soil properties and test program

3.1. Classification

The soil analyzed in this study comes from the washing sludge of a lacustrine gravel near Neuchâtel Lake (fig. 3). The properties of the soil were determined according to Swiss standards VSS and listed in table 1. The soil is composed by 3% of sand, 69% of silt and 28% of clay. According to the USCS classification, the soil is a clay loam CL. (fig. 4). The frost sensitivity is very high: G4. According to the compaction test, the maximum dry density and optimum water content are 1.831 Mg/m^3 and 14.4% respectively.

3.2.Sample preparation

In order to avoid mismatches in the results due to the natural heterogeneity of the soils, samples were prepared artificially under repeatable conditions. Thus, the variations observed between tests can be directly linked to the freeze/thaw effect. The compaction water content of the samples was set at 20% in order to obtain a degree of saturation of around 85%. Then, saturation (Sr > 95%) was completed during the first step of the triaxial test. Water was mixed with the soil powder to reach the target water content using a mechanical mixing machine. Then the soil was stored in a plastic bag until the

Tab. 1 – Physical properties of tested clay loam.

Sand [%]	Silty [%]	Clay [%]	Liquid limit [%]	Plastic limit [%]	Specific gravity [Mg/m^3]
3.0	69.4	27.6	27.2	18.5	2.74

Fig. 3 – Localisation of the gravel in Switzerland.

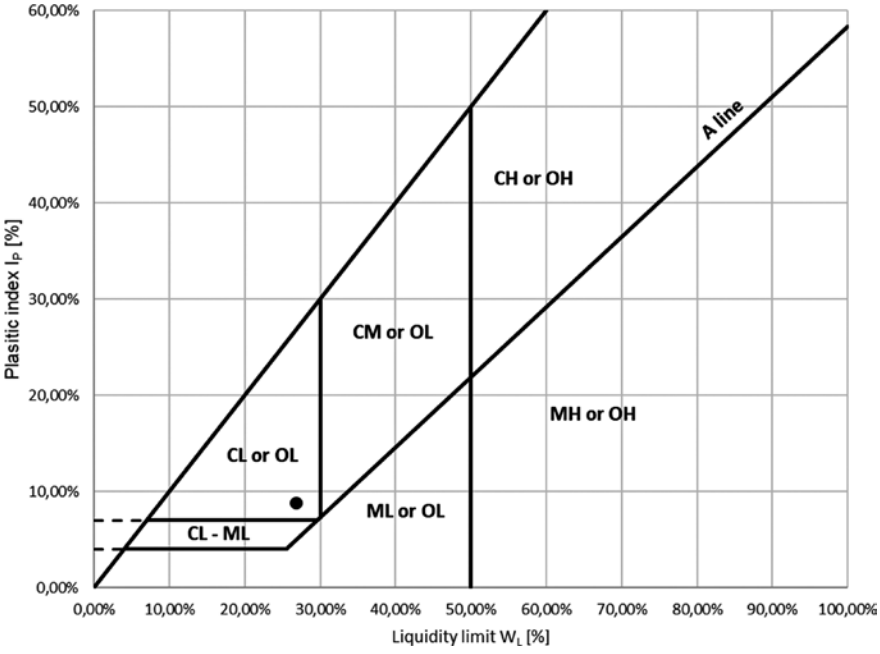

Fig. 4 – USCS classification.

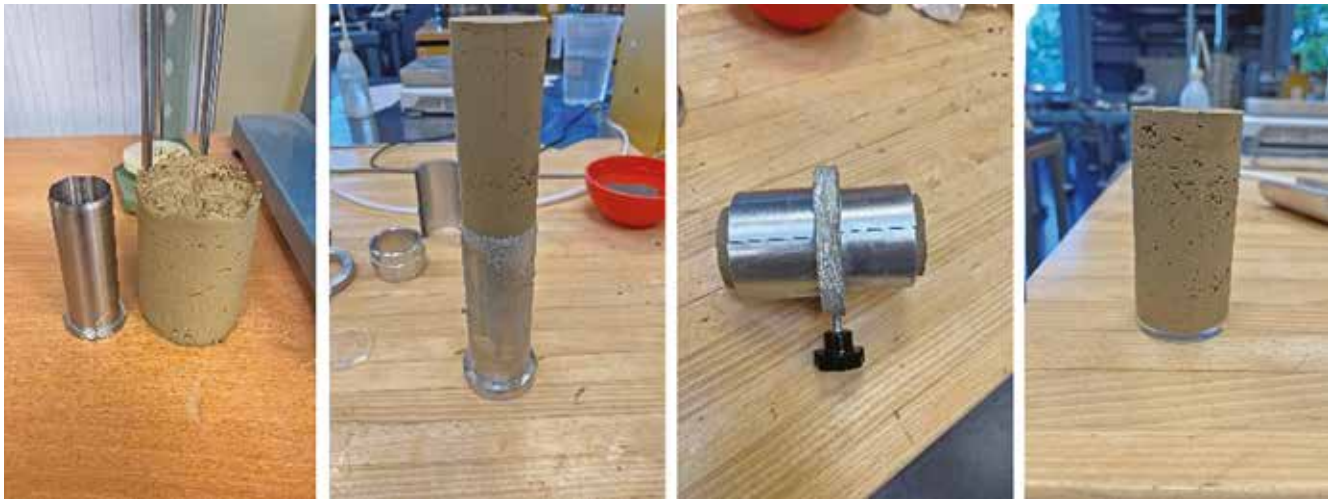

Fig. 5 – Sample preparation.

water was homogenously redistributed. The soil was compacted in a A-type Proctor mold (L = 119 mm and Ø = 101 mm) with an energy compaction of 0.6 MJ/m^3. This energy is used for the standard compaction test. Our compacter is set up for this energy, that is why we chose 0.6 Mj/m^3 compaction energy in order to limit the human error during the confection of the samples. Compaction was carried out in a mechanical compacter calibrated precisely for this energy. In that respect, the human errors during the confection of the samples were highly restrained. After extraction from the Proctor mold, the samples were cut in order to obtain a cylinder of 100 mm length and 50 mm diameter (fig. 5).

Finally, several tests were performed on artificial samples before freezing, including a CU+u triaxial test, to determine the reference properties of the specimens and are listed in table 2.

Tab. 2 – Reference properties.

γ [Mg/m^3]	w [%]	Sr [%]	e_0 [-]	c_u [kPa]	φ_u [°]
2.01	20.1	86.4	0.639	23.9	22.4

3.3. Test plan

In this study, a triaxial device with a thermal control was used to experimentally quantify the effect of thawing on the properties of frozen soils.

Initially, three triaxial tests were carried out on samples frozen at –5 °C, followed by three other tests performed at +5 °C.

The choice of the test type was therefore made for a consolidated undrained test (CU) for frozen sample and a consolidated undrained test with pore water pressure measurement (CU+u) for the thawed samples. The tests began with a step of saturation until the B check was bigger than 0.95. The cell pressure is gradually increased to 660 kPa while maintaining an effective pressure of 10 kPa. Then, samples were consolidated during 24 hours. The back pressure was maintained at 650 kPa and the cell pressure was increased to 750 kPa, 850 kPa, 1050 kPa and 1250 kPa. As these tests were innovative, we decided to use four samples per test and selected the three best Mohr circles for analyzing the results. After the consolidation step, samples were frozen at –5 °C temperature during 24 hours.

The temperature of the sample was controlled by a coil connected to the thermal controller (fig. 6). Liquid flows through the coil, heating or cooling the fluid inside the cell. The cell fluid is a mixture of demineralized water and antifreeze which helps maintain a liquid state during system cooling and facilitates the application of the cell pressure. A thermal sensor is integrated into the system to monitor the temperature of the containment fluid. After a freeze step of 24 hours at –5 °C, samples were sheared in the press at a speed of 0.02 mm/min. This speed was calculated in function of test conditions and the first curve of consolidation. The shear strength was measured every 0.1% of deformation.

For the tests after thawing, the

Fig. 6 – System assembly.

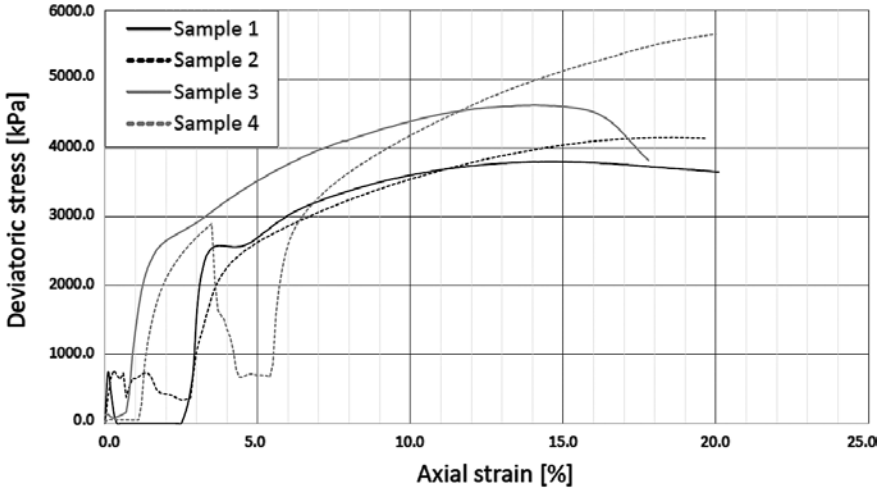

Fig. 7 – Deviatoric curves, test 1 at –5 °C.

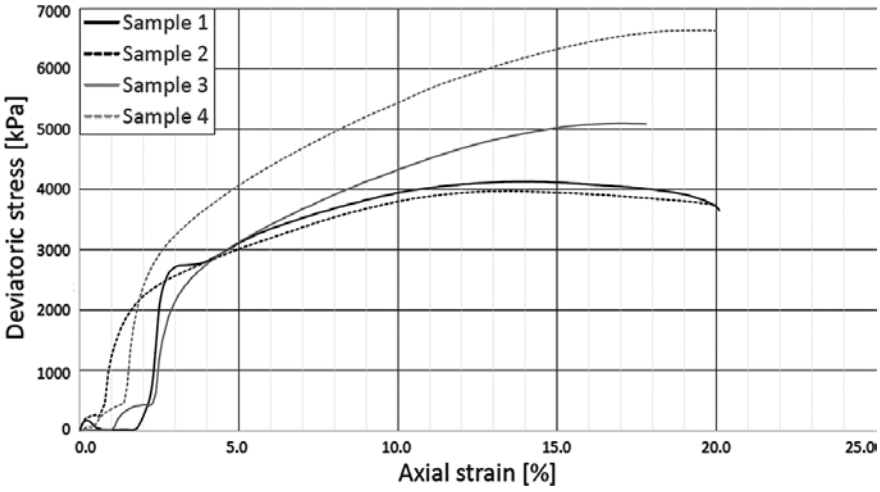

Fig. 8 – Deviatoric curves, test 2 at –5 °C.

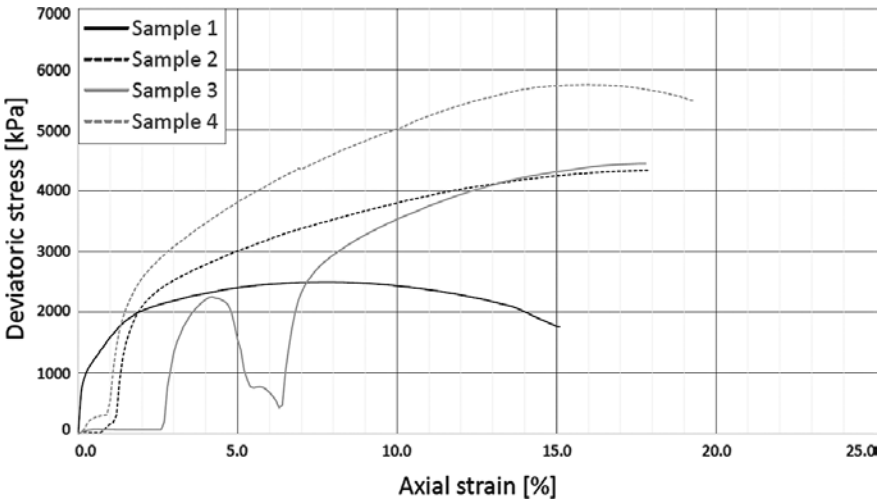

Fig. 9 – Deviatoric curves, test 3 at –5 °C.

samples were frozen following the same procedure as for the frozen tests, then thawed at +5 °C during 12 hours before shearing.

After exploitation of the shear strength curves, we were able to determine the cohesion and the internal friction angle of the soil to compare the state during and after freezing.

4. Test results

4.1. Triaxial test at –5 °C

Interpreting the results of triaxial tests on frozen soils is complicated due to ice presence in the sample. This is why interpreting the stress-strain response of the samples required making certain choices to describe the results, as a standard triaxial test interpretation was not applicable for this type of test. Since the water in the samples was in an ice state, no pore water pressure could be measured. Therefore, the calculations were performed using total stress. Moreover, we assumed that the sample was totally frozen and could be considered as an impervious rock. Thus, we considered the cell pressure as the effective pressure.

The failure criterion adopted in this study was the peak deviatoric stress, unless it was not clearly visible. In which case values of deviatoric stress at a displacement of 15% were used. Some deviatoric stress curves did not show a clear increase upon loading (fig. 7). This effect is due to the engage system of the triaxial press and was taken into account when measuring the

Tab. 3 – Raw results of tests at –5 °C.

		Effective pressure [kPa]	Deviatoric stress peak [kPa]	Axial strain peak [%]
Test 1	sample 1	750.8	3741.5	17.5
	sample 2	850.9	4148.5	17.8
	sample 3	1050.4	4559.0	15.7
	sample 4	1250.3	5262.3	16.1
Test 2	sample 1	750.7	4055.6	16.8
	sample 2	850.5	3932.9	15.7
	sample 3	1050.4	5096.8	17.2
	sample 4	1250.3	6487.9	16.4
Test 3	sample 1	750.8	2497.2	8.0
	sample 2	850.4	4303.1	16.2
	sample 3	1050.4	4449.5	17.8
	sample 4	1250.4	5479.1	16.0

peak of deviatoric stress.

As triaxial tests on frozen ground are rare, we decided to carry out four shear tests per test in case one result was inconsistent with the others. This choice proved to be very useful, because as expected, some points were discarded in order to obtain consistent results. Figures 7, 8 and 9 show the curves of deviatoric stresses. Table 3 summarises the raw results of the three triaxial tests at –5 °C.

4.2. Triaxial test at +5 °C

The analysis of these tests was more conventional. In these cases, the water inside the specimens returned to a liquid phase allowing the pore water sensor to record usable data. As for the tests conducted at –5 °C, deviatoric stress peaks were recorded at 15% displacement (with correction applied) if no peaks were initially observed. Figures 10, 11 and 12 show the curves of deviatoric stresses and table 4 summarises the raw results of the three triaxial tests at +5 °C.

Tab. 4 – Raw results of test at 5 °C.

		Effective pressure [kPa]	Deviatoric stress peak [kPa]	Axial strain peak [%]
Test 1	sample 1	99.5	295.4	17.0
	sample 2	199.7	479.4	15.7
	sample 3	399.9	845.8	19.6
Test 2	sample 1	99.8	268.8	15.6
	sample 2	199.7	467.1	15.5
	sample 3	399.8	857.5	16.3
Test 3	sample 1	99.7	262.0	16.3
	sample 2	199.8	424.0	15.7
	sample 3	399.9	808.2	17.1

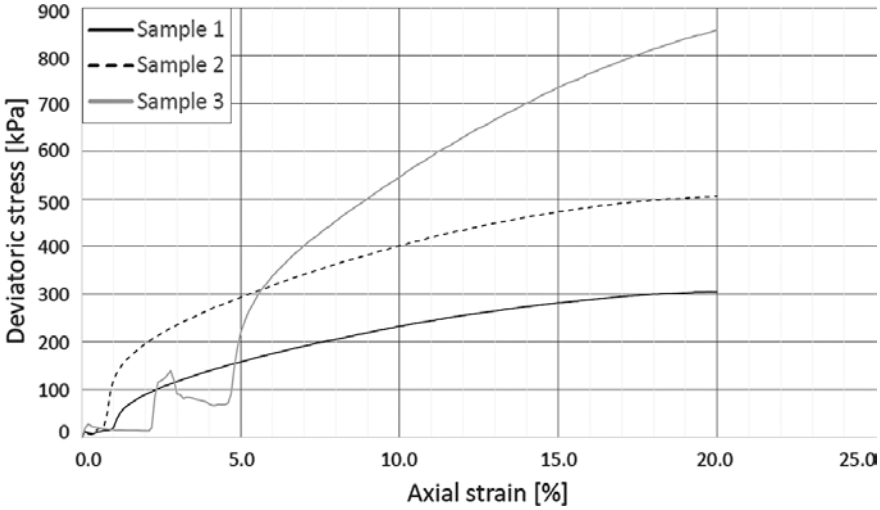

Fig. 10 – Deviatoric curves, test 1 at 5 °C.

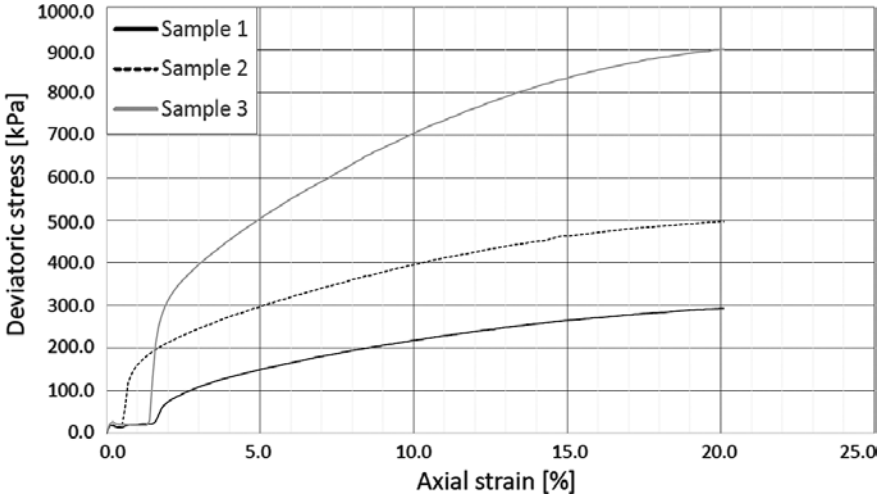

Fig. 11 – Deviatoric curves, test 2 at 5 °C.

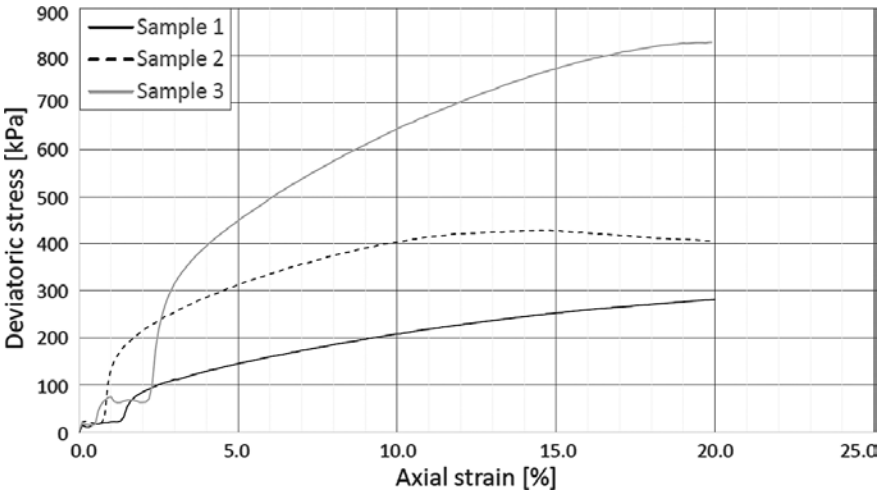

Fig. 12 – Deviatoric curves, test 3 at 5 °C.

5. Discussion

The failure behavior of the samples was generally ductile, although some samples exhibited very pronounced failure planes with a sharp drop in deviatoric stress, such as the sample at 1050kN/m^2 from test 1 at –5 °C (fig. 13), the other specimens showed predominantly a ductile failure in barreling mode.

As mentioned before, the analysis of the freezing triaxial test re-

Fig. 13 – Sample 3 of test 1 at –5 °C.

sults was difficult. Figures 14, 15 and 16 are the representation of Mohr's circles for the three tests carried out at a temperature of –5 °C. As mentioned in chapter 4, we have considered the frozen samples as a single-phase block, which implies that the cell pressure is equal to the effective pressure of the sample. For each test, sigma 3 is equal to the confining pressure and sigma 1 is the sum of sigma 3 and the deviatoric stress peak.

The difficulty arises in plotting the Mohr-Coulomb line. Mohr's circles did not align perfectly in tests 2 and 3 at –5 °C, making it challenging to draw a tangent line. In contrast, the first test at –5 °C was pretty easy to exploit.

The Mohr-Coulomb line was tangent to the four circles as shown in figure 14.

It can be seen in figure 15 that the Mohr's circle drawn with the results of sample 2 is smaller than the circle of sample 1. There were therefore two possible Mohr-Coulombs lines, the first being the tangent to circles 1, 3 and 4 and the second being the tangent to circles 2, 3 and 4. The second solution was discarded because it gave a soil cohesion value below 0 kPa, which is impossible. We can therefore conclude that the shearing of sample 2 encountered a problem that led to a low shear strength.

The analysis of the third test at –5 °C presented the greatest challenge. To visualize the issue, two Mohr Coulomb lines were drawn in figure 16. The first Mohr-Coulomb line was constructed using data from samples 1, 3 and 4. Although the line was perfectly tangent to the three circles, this line has been discarded for the fol-

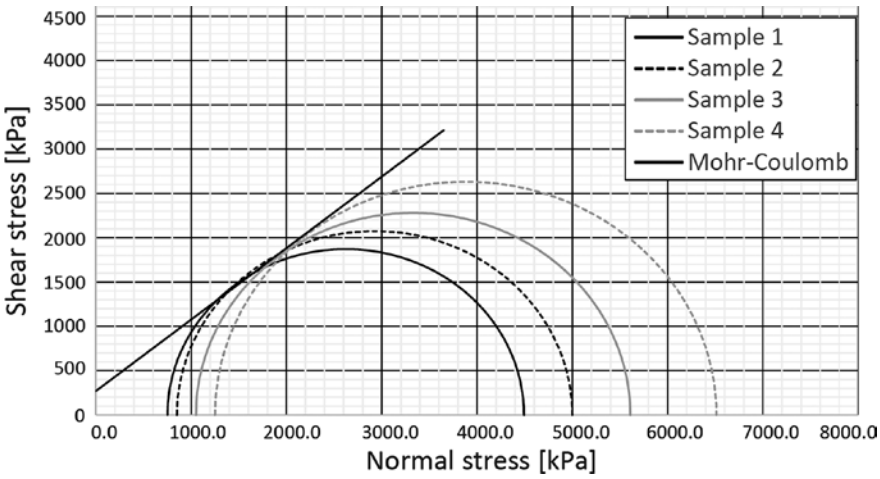

Fig. 14 – Test 1 at a temperature of –5 °C.

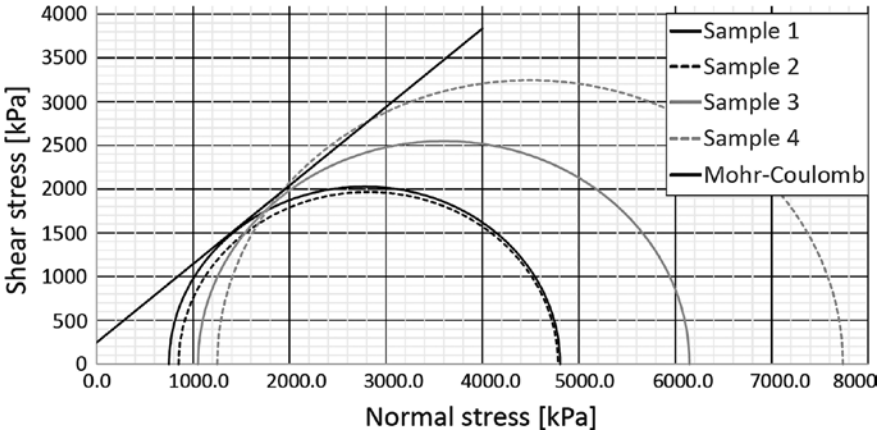

Fig. 15 – Test 2 at a temperature of –5 °C.

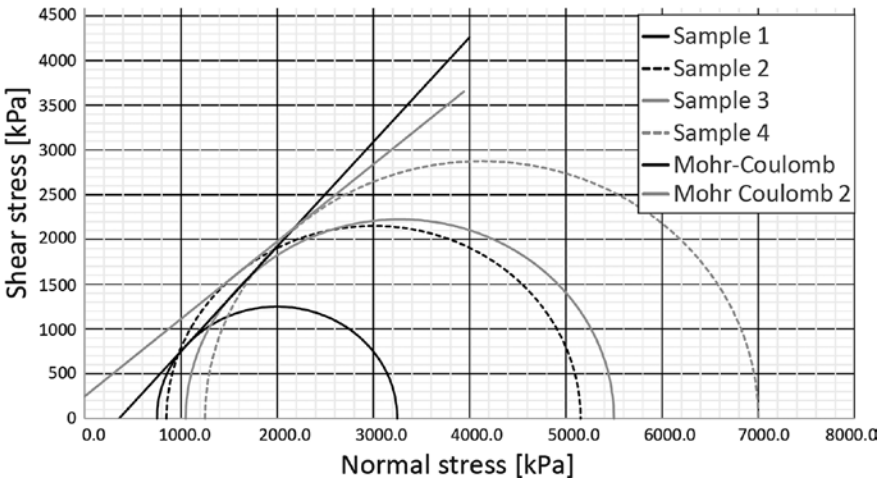

Fig. 16 – Test 3 at a temperature of –5 °C.

lowing reasons. Firstly, the deviatoric stress curve of sample 1 exhibited an unusual pattern, with the deviatoric stress peak occurring at an 8% axial strain rate. This value is abnormally low compared to all other tests, roughly half as much and there is no clear evidence of failure. It is likely that the sample had a design flaw, resulting in low shear strength. Secondly, the circle from the results of the third sample is clearly not usable. We can see on figure 16 that the Mohr's circle is smaller than sample 2 for a higher effective stress. This is probably due to the pre-failure visible on figure 9 at 4.5% of deformation. Thirdly, the first Mohr-Coulomb line was not correct because it led to a negative cohesion. That is why we have drawn a second Mohr-Coulomb line tangent to the circles 2 and 4. This line led to a realistic result.

Table 5 summarizes the results of the tests at –5 °C. The results of cohesion and internal friction angle are very similar for the three tests. As expected, the cohesion of the soil increased a lot during the freezing phase. Compared to its initial state, the cohesion of the soil is 10.6 times higher and the internal friction angle is 1.8 times higher. The phase change in soil significantly impacts its mechanical properties.

Tab. 5 – Summary of cohesion and friction angle during freezing.

	Cohesion [kPa]	Internal friction angle [°]
Test 1	268.97	38.89
Test 2	245.47	41.91
Test 3	246.95	40.84
Mean	253.80	40.55
Standard deviation	13.16	1.53

Analyzing the test after the freezing cycle at –5 °C and subsequent thawing at +5 °C did not pose significant difficulties. The alignment of the Mohr-Coulomb lines is almost perfect on all three tests (fig. 17, 18 and 19). On top of that, no anomalies have been detected on the deviatoric curves.

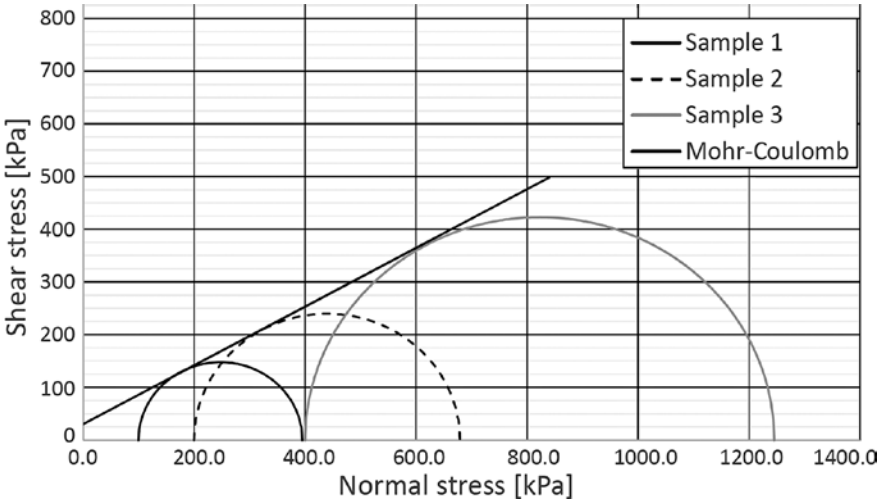

Fig. 17 – Test 1 at a temperature of 5 °C.

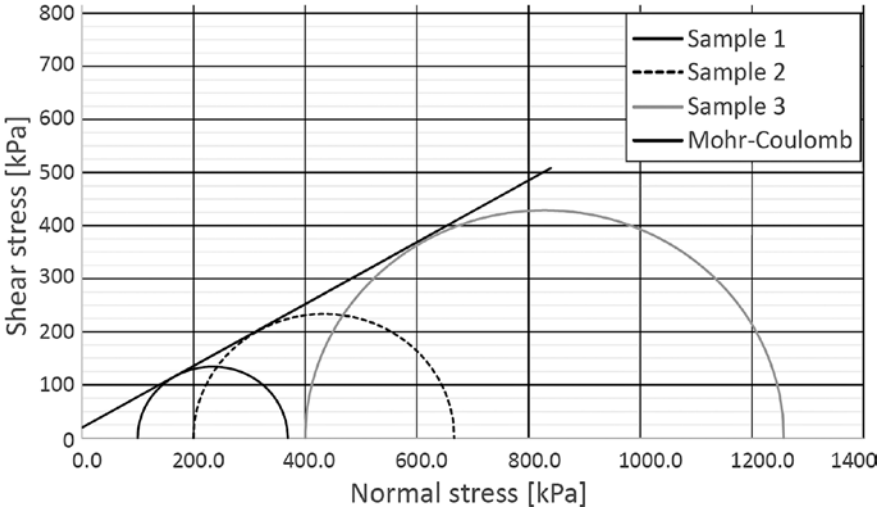

Fig. 18 – Test 2 at a temperature of 5 °C.

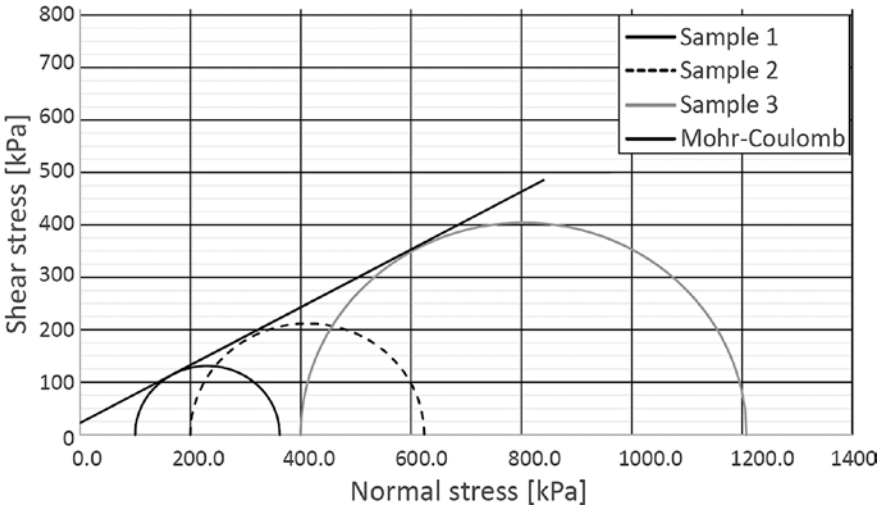

Fig. 19 – Test 3 at a temperature of 5 °C.

Table 6 summarizes the results of the tests at +5 °C. The first ob-

servation that we could do is the strong decrease of cohesion and internal friction angle after the specimens thawed. Compare to its frozen state, the soil cohesion has decreased by a factor of 10 during the thawing step. The interesting thing is that the cohesion seems to return to its initial value before any freeze/thaw effect even if the value is slightly higher than the initial state. We can, however, question the significance of this increase. Indeed, the initial cohesion of the soil is close to the average value after thawing. Moreover, the standard deviation of the cohesion is quite high and covers the difference between the two values.

Although the effect of one freeze / thaw cycle does not seem to affect significantly the cohesion value, the same is not true for the internal friction angle. Strong changes in the value of the internal friction angle can be identified in all states. When the sample is frozen, friction angle increases by about 81% compared to its initial state. Then during thawing, friction angle decreases by 27.4%. However, after the freeze-thaw cycle, the value of friction angle remains about 30% higher than its pre-freeze state. The results obtained by the six tests (3 during freezing, 3 after thawing) are very close and the standard deviations are low. A phenomenon in the soil occurs during freezing that permanently alters their initial internal friction angle. We can propose various hypotheses regarding its origin. A probable rearrangement of the solid skeleton during the gel phase is one of them. To determine more precisely the cause of this phenomenon, further studies are necessary.

It should also be noted that when the soil goes from the frozen to the thawed state, its mechanical properties decrease very sharply (approximately 10-fold decrease in cohesion and 30% decrease in friction angle). These changes lead to a sharp decline in the bearing capacity of the soil. The loss of bearing capacity also depends on other factors that are specific to each infrastructure (type of foundation, depth of foundation etc.) and therefore cannot be accurately quantified in a general way.

Tab. 6 – Summary of cohesion and friction angle after thawing.

	Cohesion [kPa]	Internal friction angle [°]
Test 1	30.54	29.12
Test 2	17.64	30.39
Test 3	22.60	28.84
Mean	23.59	29.45
Standard deviation	6.51	0.83

6. Conclusion

This study aimed to experimentally quantify the effect of thawing on a reconstituted soil's geomechanical strength. For this purpose, a classification of soil geomechanical parameters was first established to serve as a reference point. Then, three triaxial shear tests at a temperature of –5 °C were performed. This temperature was chosen to be slightly lower than that measured in permafrost monitoring boreholes in the Alps (Switzerland and France). Three additional tests were carried out at a temperature of 5 °C after being frozen for 24 hours at a temperature of –5 °C.

These tests highlighted the importance of soil condition (frozen/thawed) on soil cohesion. Indeed, cohesion varies by a factor of 11 between these two states. Nevertheless, the value of the cohesion seems to return to its initial state after thawing. Soil cohesion seems to depend only on the state of the soil (frozen/thawed) but it would be interesting to perform additional tests at different temperatures to confirm this hypothesis.

The variation in the soil's friction angle is less pronounced than that in cohesion. When the soil thaws, friction angle decreases by about 30% of its value. It should be noted that this angle increases sharply when the soil is frozen (+81% compared to its initial state). The most surprising thing is that the value of friction angle does not return to its initial state, unlike cohesion. This may indicate two things:

Either the freeze-thaw cycle causes a fundamental change in soil properties. The soil cannot return to its original mechanical properties.

Either the mechanical parameters of the soil are strongly temperature dependant.

Or a combination of these two facts.

This study should also be completed with additional tests at other temperatures to verify these hypotheses.

Understanding the impacts of permafrost thaw is complex. That is why, further studies on this topic are strongly recommended. The more studies are carried out on the subject, the more we will be able to understand the impact of global warming on permafrost, and therefore the impact on human kind and its environment.

References

Arenson, L., Hoelzle, M., Springman, S., (2002). Borehole deformation measurements and internal structure of some rock glacier in Switzerland. Permafrost and periglacial processes, Volume 13, pp. 117-135. https://doi.org/10.1002/ppp.414

Arenson, L., Springman, S., (2005). Mathematical descriptions for the beha-

viour of ice-rich frozen soils at temperatures close to 0 °C. Canadian Geotechnical Journal, pp. 431-442. https://doi.org/10.1139/t04-109

Bardou, E., Favre-Bulle, G., Ornstein, P., Rouiller, J.-D., (2011). Influence of the connectivity with permafrost on the debris-flow triggering in high-alpine environment. Engineering Geology and the Environment, Volume 10, pp. 13-21. https://doi.org/10.4408/IJEGE.2011-03.B-002

Blikra, L.H., Christiansen, H.H., (2014). A filed-based model of permafrost-controlled rockslide deformation in northern Norway. Geomorphology, Volume 208, pp. 34-49. https://doi.org/10.1016/j.geomorph.2013.11.014

Chamberlain, E., Gow, A., (1979). Effect of Freezing and Thawing on the Permeability and Structure of Soils. Developments in Geotechnical Engineering, Volume 26, pp. 73-92. https://doi.org/10.1016/B978-0-444-41782-4.50012-9

Damm, B., Felderer, A., (2013). Impact of atmospheric warming on permafrost degradation and debris flow initiation – a case study from the eatern European Alps. *Quaternary Science journal,* 62(2), pp. 136-149. https://doi.org/10.3285/eg.62.2.05

Ding, Y. *et al.*, (2019). Global warming weakening the inherent stability of glaciers and permafrost. *Science bulletin,* Volume 64, pp. 245-253. https://doi.org/10.1016/j.scib.2018.12.028

Dysli, 1993. *Where does the water go during ice lenses thaw?.* Anchorage, s.n., pp. 45-50.

Etzelmüller, B., Berthling, I., Sollid, J.L., 2003. Aspects and concepts on the geomorphological significance of Holocene permafrost in southern Norway. *Geomorphology,* Volume 52, pp. 87-104. https://doi.org/10.1016/S0169-555X(02)00250-7

Farbrot, H., Isaksen, K., Etzelmüller, B., Gisnas, K., (2013). Ground thermal regime and permafrost distribution under a changing climate in Northern Norway. *Permafrost and periglacial processes,* Volume 24, pp. 20-38. https://doi.org/10.1002/ppp.1763

Frauenfelder, R., Isaksen, K., Matthew, J.L., Noetzli, J., (2018). Ground thermal and geomechanical conditions in a permafrost-affected high-latitude rock avalanche site (Polvartinden, northern Norway). *The cryosphere,* Volume 12, pp. 1531-1550. https://doi.org/10.5194/tc-12-1531-2018

Guo, D., Wang, H., Li, D., (2012). A projection of permafrost degradation on the Tibetan Plateau during the 21st century. *Journal of Geophysical research,* Volume 117. https://doi.org/10.1029/2011JD016545

Haeberli, W., (1992). Construction, Environmental problems and natural hazards in periglacial mountain belts. *Permafrost and periglacial processes,* Volume 3, pp. 111-124. https://doi.org/10.1002/ppp.3430030208

Hilger, P. *et al.*, (2021). Permafrost as a first order control on long-term rock.slope deformation in (Sub-) Arctic Norway. *Quaternary Sciences Reviews,* Volume 251. https://doi.org/10.1016/j.quascirev.2020.106718

Hipp, T., Etzelmüller, B., Farbrot, H., Schuler, T.V., (2011). Modelling the temperature evolution of permafrost and seasonal frost in southern Norway during the 20th and 21st century. *The cryosphere discussions,* Volume 5, pp. 811-854. https://doi.org/10.5194/tcd-5-811-2011

Isaksen, K. *et al.*, (2011). Degrading mountain permafrost in Southern Norway : spatial and temporal varaibility of mean ground temperatures, 1999-2009. *Permafrost and Periglacial Processes,* Volume 22, pp. 361-377. https://doi.org/10.1002/ppp.728

Isaksen, K. *et al.*, (2002). Mountain permafrost distribution in Dovrefjell and Jorunheimen, southern Norway, based on BTS and DC resistivity tomography data. *Norwegian journal geography,* 56(2), pp. 122-136. https://doi.org/10.1080/00291950276005645 9

Isaksen, K., Holmlund, P., Sollid, J.L., Harris, C., (2001). Three deep alpine-permafrost boreholes in Svalbard and Scandinavia. *Permafrost and periglacial processes,* Volume 12, pp. 13-25. https://doi.org/10.1002/ppp.380

Lyon, C. *et al.*, (2022). Climate change research and action must look beyond 2100. *Global Change Biology,* Volume 28, pp. 349-361. https://doi.org/10.1111/gcb.15871

Matthews, J.A. *et al.*, (2018). Small rock-slope failures conditioned by Holocene permafrost degradation: a new approach and conceptual model based on Schmidt-hammer exposure-age dating, Jotunheimen, southern Norway. *An international journal of quaternary research,* Volume 47, pp. 1144-1169. https://doi.org/10.1111/bor.12336

Myhra, K.S., Westermann, S., Etzemüller, B., (2017). Modelled distribution and temporal evolution of permafrost in steep rock walls along a latitudianal transect in Norway by CryoGrid 2D. *Permafrost and Periglacial Processes,* Volume 28, pp. 172-182. https://doi.org/10.1002/ppp.1884

Perov, V., Chernomorets, S., Budarina, O., (2017). Debris flow hazards for mountain regions of Russia: regional features and key events. *Springer,* pp. 199-235. https://doi.org/10.1007/s11069-017-2841-3

Prina Howald, E., Bonnard, C., Laloui, L., (2016). TR3 project: slope safety preparedness for effects of climate change contribution for Switzerland. Dans: H. Ken, S. Lacasse, L. Picarelli, éds. Slope Safety Preparedness for Impact of Climate Change. London: CRC Press. https://doi.org/10.1201/9781315387789

Prina Howald, E., Torche, J., (2020). Global warming and loss of bearing capacity of permafrost : an experimental study on the effects of freezing/thawing cycles on a silty soil. *Global Journal of Earth Science and Engineering,* Issue 7, pp. 1-21.

Saemundsson, P. *et al.*, (2018). The triggering factors of the Moafellshyrna debris slide in northern Iceland : intense precipitation, earthquake activity and thawing of mountain permafrost. *Science of the total en-*

vironment, Volume 621, pp. 1163-1175. https://doi.org/10.1016/j.scitotenv.2017.10.111

Sattler, K., Keiler, M., Zischg, A., Schrott, L., (2011). On the connection between debris flow activity and permafrost degradation: a case study from the schnalstal, South Alps, Italy. *Permafrost and periglacial precesses,* Volume 22, pp. 254-265. https://doi.org/10.1002/ppp.730

Stoffel, M., Bollschweiler, M., Beniston, M., (2011). Rainfall characteristics for periglacial debris flows in the Swiss Alps: past incidences – potential future evolutions. *Climatic Change,* Volume 105, pp. 263-280. https://doi.org/10.1007/s10584-011-0036-6

Torche, J., Prina Howald, E., (2017). Influence of the climate change on the evolution of soil bearing capacity : an experimental study on the effects of freezing/thawing cycles. *IX Simposio Nacional sobre Taludes y Laderas Inestables,* pp. 295-306.

Zhang, Y., Chen, W., Riseborough, D.W., (2008). Transient projections of permafrost distribution in Canada during 21st century under scenarios of climate change. *Global and Planetary Change,* Volume 60, pp. 443-456. https://doi.org/10.1016/j.gloplacha.2007.05.003